

Possible Bose-Einstein condensate of magnons in single-crystalline $\text{Pb}_2\text{V}_3\text{O}_9$ B. S. Conner,^{1,2} H. D. Zhou,^{1,2} Y. J. Jo,^{2,*} L. Balicas,² C. R. Wiebe,^{1,2,†} J. P. Carlo,³ Y. J. Uemura,³ A. A. Aczel,⁴ T. J. Williams,⁴ and G. M. Luke⁴¹*Department of Physics, Florida State University, Tallahassee, Florida 32306-3016, USA*²*National High Magnetic Field Laboratory, Florida State University, Tallahassee, Florida 32306-4005, USA*³*Department of Physics, Columbia University, New York, New York 10027, USA*⁴*Department of Physics and Astronomy, McMaster University, Hamilton, Ontario, Canada L8S 4M1*

(Received 8 June 2009; revised manuscript received 4 January 2010; published 7 April 2010)

We report the growth and the characterization of single crystals of the $S=1/2$ spin-dimer compound $\text{Pb}_2\text{V}_3\text{O}_9$. Magnetic-susceptibility, torque magnetometry, heat-capacity, and muon-spin-relaxation measurements provide evidence for a field-induced Bose-Einstein condensate of magnons in this system. At low temperatures, the field-dependent phase boundary between the dimerized and the condensed state is well described by the expression $T^* \propto (H - H_{c1})^{1/\phi}$, with $\phi = (2.00 \pm 0.04)$.

DOI: [10.1103/PhysRevB.81.132401](https://doi.org/10.1103/PhysRevB.81.132401)

PACS number(s): 75.30.Kz, 03.75.Nt, 75.45.+j

The fundamental discovery of Bose-Einstein condensates (BECs) (Refs. 1 and 2) led to a deeper understanding of exotic ground states in strongly correlated systems. The superfluid transition in liquid ^4He is perhaps the most celebrated example of how an interacting system of bosons can give rise to a macroscopically degenerate quantum ground state with unique properties.³ In the last few decades, BECs have been observed in variety of systems, ranging from ultracold atoms to exotic superconductors.⁴ The idea of a zero resistance ground state formed by bosonic Cooper pairs of quasiparticles persists as the fundamental concept for a comprehensive theory of superconductivity.⁵

One of the current challenges in condensed-matter physics is to find unambiguous magnetic analogs of BECs arising from the condensation of integer spin excitations or magnons.⁶ A BEC transition cannot occur in a system purely composed of one-dimensional (1D) chains, even at zero temperature, since the bosonic excitations would not freely propagate throughout the system. Nonetheless, convincing evidence for these phase transitions has been reported in spin-chain systems such as TiCuCl_3 .⁷ Theoretical work suggests that only very weak coupling is needed between the chains to allow the formation of a BEC state.^{8,9}

In this Brief Report, we present evidence for a BEC of magnons in single-crystalline $\text{Pb}_2\text{V}_3\text{O}_9$. This compound is composed of isolated spin dimer chains of V^{4+} ($S=1/2$) ions, with no evidence of a bulk phase transition down to 20 mK in zero field. In applied fields, the Zeeman splitting of the excited triplet state reduces the singlet-triplet excitation energy and induces a transition to a possible BEC that was first documented by Waki *et al.*¹¹ However, the initial reports on this material were made on polycrystalline samples and the power-law description of the phase boundary could not confirm that a BEC-type state indeed exists. We have recently grown single crystals of $\text{Pb}_2\text{V}_3\text{O}_9$ to resolve this controversy, characterizing the magnetic properties through dc susceptibility, torque-magnetometry, heat-capacity, and muon-spin-relaxation (μSR) experiments.

Polycrystalline $\text{Pb}_2\text{V}_3\text{O}_9$ was synthesized via the following reaction: high purity V_2O_5 and PbO were ground and then heated up to 875 K in flowing Ar gas for 2 days to make

$\text{Pb}_2\text{V}_2\text{O}_7$ (the mineral chervetite). The chervetite was subsequently ground with high purity VO_2 and heated in an evacuated quartz ampoule at 975 K for three days. The resulting compound is stoichiometric $\text{Pb}_2\text{V}_3\text{O}_9$. The purity of the obtained phase was verified to a few percent by x-ray diffraction measurements. The room-temperature x-ray powder diffraction pattern was obtained by using the $\text{Cu } K_{\alpha 1}$ (1.54059 Å) radiation line. The x-ray data was fitted by using the FULLPROF software. Finally, single crystals of $\text{Pb}_2\text{V}_3\text{O}_9$ were synthesized via the floating-zone technique: the polycrystalline powder was pressed into rods and melted in the focused radiation of an image furnace at the National High Magnet Field Laboratory (NHMFL). A photograph of one of such crystal is shown in Fig. 1(a). $\text{Pb}_2\text{V}_3\text{O}_9$ crystallizes in the triclinic space group $\text{C}\bar{1}$.¹⁰ The x-ray diffraction pattern fit returns lattice parameters $a=7.6010(15)$ Å, $b=16.4166(27)$ Å, $c=6.9729(12)$ Å, $\alpha=91.33(2)^\circ$, $\beta=119.38(1)^\circ$, and $\gamma=90.50(2)^\circ$. The V^{4+} ($S=1/2$) spins are surrounded by oxygen atoms, forming corner sharing octahedra. These octahedra form chains along the [101] direction with alternating V^{4+} interatomic distances [Fig. 1(a)] that are responsible for the dimer description. The interchain distances are 8.9(1) Å and 7.0(1) Å, respectively. The two nonmagnetic V^{5+} atoms sit in oxygen tetrahedra that share corners with the V^{4+} octahedra.

dc magnetic-susceptibility measurements were performed on a ground single crystal with a superconducting quantum interference device from 5 to 270 K in an applied magnetic field of 1 T. Specific-heat measurements were performed on a single-crystalline sample in applied fields up to 9 T. The applied magnetic field was varied from 0 to 9 in 0.25 T increments. The crystalline [101] direction was aligned parallel to the applied field. Torque magnetometry measurements were performed on single-crystalline $\text{Pb}_2\text{V}_3\text{O}_9$ in a ^3He refrigerator and under fields up to 35 T at the NHMFL. The sample was mounted onto a CuBe cantilever with the external field applied at a small angle with respect to the crystalline [101] direction. Temperature sweeps were performed under fixed values of the applied field. Muon-spin-relaxation measurements were completed on the M15 beamline at TRIUMF (Vancouver, Canada) using a dilution fridge

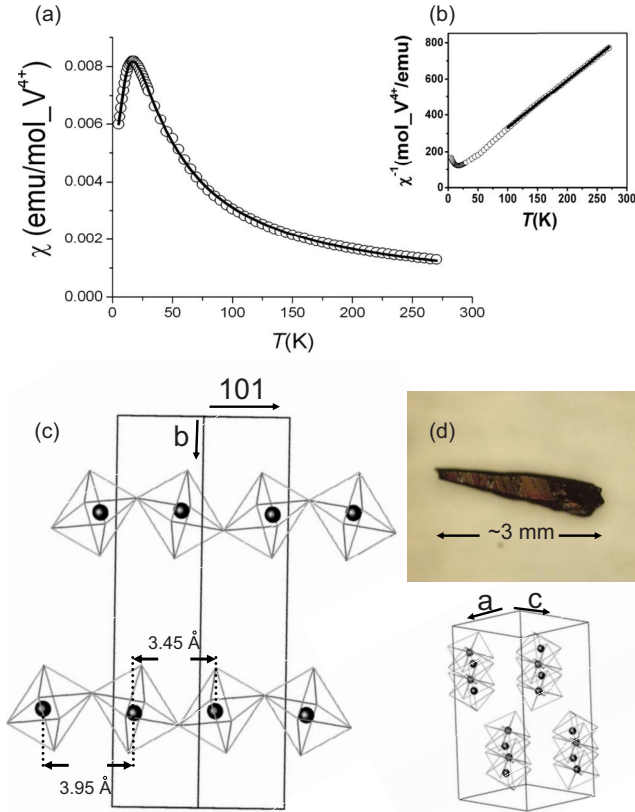


FIG. 1. (Color online) (a) $\text{Pb}_2\text{V}_3\text{O}_9$ structure and photograph. (b) Temperature dependence of the magnetic susceptibility. Open circles represent experimental data points. The solid line represents the alternating chain fit of Ref. 12. The reciprocal of χ is displayed in the inset with the solid line representing a Curie-Weiss fit.

with a base temperature of 0.02 K and a maximum applied transverse field (TF) of 6 T. Aligned single crystals were mounted with the chain direction perpendicular to the applied field.

The inverse of the dc magnetic susceptibility, $\chi^{-1}(T)$, is displayed in the inset of Fig. 1(b). For $T \geq 100$ K, this trace was fitted to the Curie-Weiss law: $\chi^{-1}(T) = (T - \theta_{\text{CW}})/C$. The resulting Curie constant, $C = N g_{\text{eff}}^2 \mu_B^2 / 3k_B = 0.382(1)$ emu/(K mol), was obtained from the slope. This corresponds to an effective moment of value $g_{\text{eff}} = 1.747(3)\mu_B$. Refs. 10 and 11 obtain $C = 0.383$ emu/(K mol) or $g_{\text{eff}} = 1.75\mu_B$ and $C = 0.368$ emu/(K mol) or $g_{\text{eff}} = 1.72\mu_B$, respectively. From the linear fit, one obtains a Curie temperature, $\theta_{\text{CW}} = -26.4(7)$ K, which is not in exact agreement with the values reported in Ref. 10 and 11. This apparent discrepancy could be attributed to the different range of temperatures used for the fits. The magnitude of θ_{CW} increases as the low end of the fitting range is increased toward room temperature. For example, for the $T = 200$ K to 270 K range one obtains $\theta_{\text{CW}} = -36(2)$ K from the fit. In fact, the inverse susceptibility is not quite linear in any range of temperatures. The lack of validity of the Curie-Weiss description is not surprising since the system consists of interacting quasi-1D moments.

A typical dc magnetic-susceptibility [$\chi(T)$] trace is shown in Fig. 1(b). The data was fitted to the alternating chain

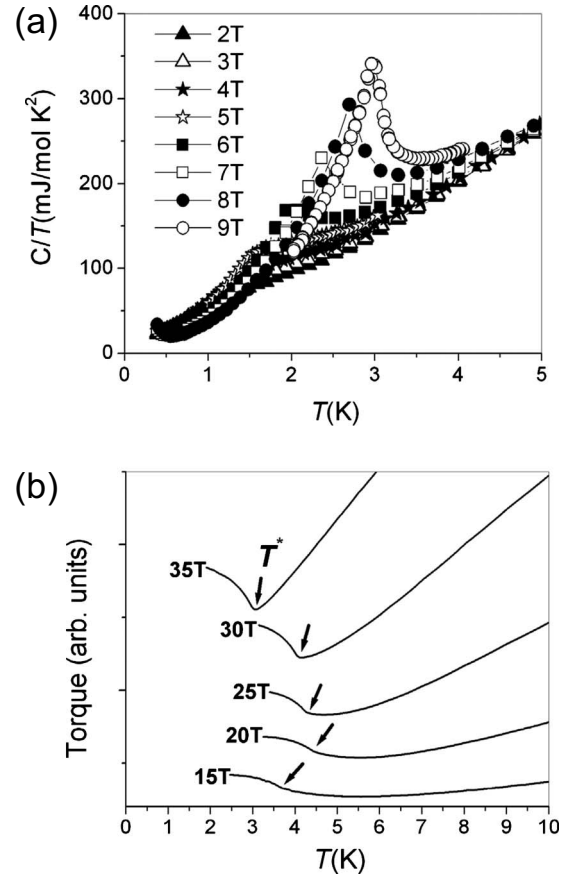


FIG. 2. (a) Temperature dependence of $C_p(T)/T$ for $\text{Pb}_2\text{V}_3\text{O}_9$. The solid lines are meant as guides to the eye. (b) Temperature dependencies of torque, in arbitrary units, for varying applied magnetic fields. T^* is determined from the second derivatives.

model of Ref. 12 with an additional term $C_{\text{imp}}/(T - \theta_{\text{imp}})$ to account for the presence of a small amount of surface impurities. Also, a small diamagnetic contribution from lead and oxygen atoms was subtracted from the data. The nearest-neighbor exchange constant is $J/k_B = -18.5(1)$ K, as determined from the fit. Refs. 10 and 11 obtain $J/k_B = -29.2$ K and -29.0 K, respectively. The interactions in these samples appear to be slightly weaker than previously reported in powder samples. The next-nearest-neighbor exchange term, J' , is determined via the parameter $\alpha = J'/J$. It may vary from 0 (noninteracting dimers) to 1 (uniform 1D spin chain). The fit yields a value $\alpha = 0.48(5)$ or $J' = -8.9(1.0)$ K. Refs. 10 and 11 obtain α values of 0.66 and 0.65, respectively. The smaller value of α obtained here suggests a more dimerized system. The energy associated with the spin gap can be estimated from J and from α (Ref. 13) and is $\Delta/k_B = 12.5$ K. This is in reasonable agreement with a previously reported value of 14.7 K, despite the differences in J and α . We note that our measurements were performed on single-crystalline samples which may account for these differences.

The temperature dependence of the specific heat divided by the temperature, $C_p(T)/T$, is plotted in Fig. 2(a). The emergence of a λ -like anomaly is observed as the applied field is increased. The ordering temperature for a given value of the applied field was determined from the position of the

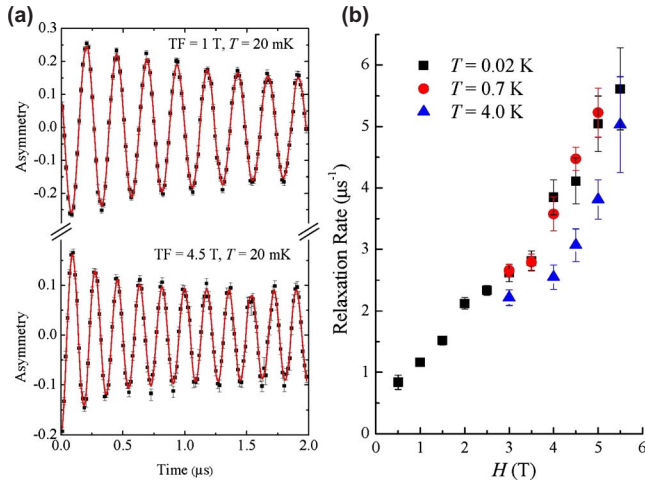


FIG. 3. (a) (Color online) Asymmetry plots of the TF muon-spin-relaxation spectrum for single-crystalline $\text{Pb}_2\text{V}_3\text{O}_9$ at applied fields of 4.5 and 1.0 T at 0.02 K. (b) Relaxation as a function of field for $T=0.02$ K, $T=0.70$ K, and $T=4.0$ K.

λ peak. However, the lower field data close to H_{c1} shows a broad feature whose maximum is more difficult to determine. For $H \geq H_{c1}$ the transition is not as well defined as the high-field data due to the low density of magnons. Consequently, the specific-heat measurements were not used to define the phase boundary for $H \leq 4.75$ T. Future specific-heat measurements at fixed temperatures and varying applied fields may be used to determine transition temperatures for lower fields.

Torque magnetometry as a function of temperature and under field, i.e., $\tau(T, H)$, is presented in Fig. 2(b). Upon entering the magnetically ordered state, one expects to observe a significant change in the magnetic response of the system, namely, a change in the slope of the temperature dependence of the torque. Kinks in $\tau(T, H)$ are clearly observable in the high-field data presented in Fig. 2(b). We use sharp features in $\partial^2 \tau(T) / (\partial T)^2$ to determine the phase boundary between the dimerized and the BEC state. For $H < 15$ T the torque data showed only very broad features which could not be used to precisely map the phase boundary. However, the combination of torque and heat capacity reveals a domelike phase diagram with a maximum $T_c \approx 4$ K at 20 T.

μSR measurements were completed at TRIUMF at dilution fridge temperatures with the initial spin of the muon polarized perpendicularly to the applied fields (TF geometry). The characteristic response was fit to an exponentially decaying function together with a nonrelaxing background function to account for the sample mount. Representative asymmetry scans are shown in Fig. 3(a). Note the significant relaxation at high fields, as expected. Using a rotating reference frame, the data was analyzed at various temperatures in fields up to 6 T. The counting times above 5 T become very long due to the increased curvature of the positron paths after muon decay and the timing resolution at high fields suffers (which are the reasons for the larger error bars in the high-field data). Nonetheless, at low temperatures a significant change in the relaxation rate is observed above 4 T. We consider this anomalous increase in the relaxation as indicative of the phase boundary. In Fig. 4, we have plotted the

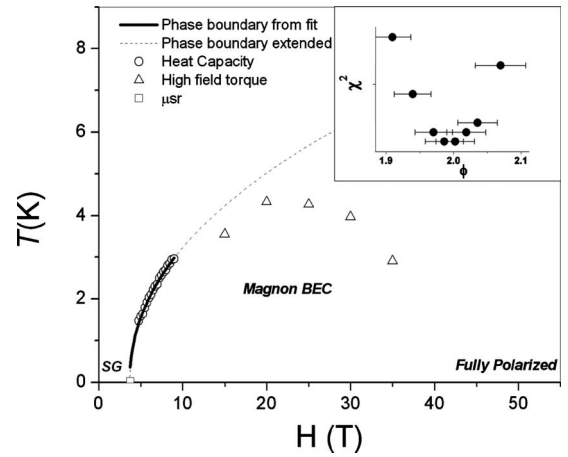


FIG. 4. Temperature-field phase boundary. In this range of temperatures the error bars in the specific heat, used to determine T_c , are smaller than the actual size of the symbols. The spin-gapped (SG), BEC of magnons, and fully polarized states are shown. The low-temperature behavior of the phase boundary between SG and BEC states is described by the power law $T^* \propto (H - H_{c1})^{1/\phi}$ with $\phi = 2.00(4)$.

temperature-field phase boundary as determined by the well-defined peaks in the heat capacity. When this data is fit and extrapolated to $T=0$ K, the field intercept, $H_{c1}(T=0$ K), is very close to the measured field value where the relaxation in the (μSR) experiments is found to increase. However, this change in relaxation rate seems to persist all the way up to ~ 4 K in fields between 3.5 and 4 T, suggesting the existence of a nearly vertical line in the phase diagram which is reminiscent of a similar feature at $H \leq H_{c1}$ reported for the $S=1$ system $\text{Ba}_3\text{Mn}_2\text{O}_8$.¹⁴ In the past, other BEC candidates have been investigated using μSR , including TlCuCl_3 ,^{15–18} but there has not been a clear determination of phase boundaries as in our experiments.

Figure 4 shows a plot of the T - H phase diagram including points from all three techniques described above. The specific-heat data from 4.75 to 9 T was used to fit the phase boundary between dimerized and BEC states to the expression $T^* = C(H - H_{c1})^{1/\phi}$. The determination of the critical exponent was completed in the following manner: the parameter H_{c1} was initially set fixed and varied in small increments of 0.05 T as the exponent was fit. The advantage here is that one fit parameter is now set fixed, reducing the overall error. This yielded a minimum in the $\chi^2/(\text{degrees of freedom})$ at a value of 3.5 T. The exponent was found to be $\phi = 2.00 \pm 0.04$.

There are numerous predictions for the value of the power law near the phase boundary. Early experiments on another BEC candidate, TlCuCl_3 , revealed a measured power law of $\phi = 2.2$.¹⁹ The value of this exponent has been a matter of debate for nearly a decade. Those authors' (Ref. 19) Hartree-Fock calculations assuming a simple quadratic dispersion of the excitation spectrum within the BEC state resulted in a power law of $\phi = 1.5$. In the same compound a recent magnetization study down to very low temperatures found that with decreasing temperature fitting range the critical exponent ϕ decreases and indeed converges to the value 1.5.²⁰

Given the TlCuCl_3 example, it is possible that one would need thermodynamic measurements down to very low temperatures to determine the precise value of ϕ for $\text{Pb}_2\text{V}_3\text{O}_9$. At lower temperatures, our attempts to determine the phase boundary precisely by thermodynamic means failed due to the fact that the transition becomes extremely weak for reasons that remain unclear. Future Faraday magnetometry experiments and a varying window analysis scheme, as in Ref. 20, may well show that ϕ converges to a universal value of 1.5 in the low-temperature limit. Although, Crisan *et al.*²¹ revisited this problem using a renormalization-group approach at the quantum phase transition and calculated a value of $\phi=2$, which is more consistent with our current results.

Finally, we comment here on the previous work to characterize the phase boundary by Waki *et al.*¹¹ on powder samples of $\text{Pb}_2\text{V}_3\text{O}_9$. Using specific-heat and susceptibility measurements, the phase boundary was characterized down

to 1.5 K. Unfortunately, the scatter in the data could not be used to reliably determine the power-law dependence, which varied in their manuscript between $\phi=1.5$ and $\phi=3.0$, with a best fit of $\phi=1.9$. Our results on high-quality single crystals put more severe constraints on the identity of the field-induced phase, which may be a BEC of magnons, possibly with a critical exponent $\phi=2.00 \pm 0.04$.

This work was made possible by support through the NSF (Grants No. DMR-0084173, DMR-0502705, and DMR-0502706), the NHMFL-UCG, the NHMFL-Schuller Program, DOE-Basic Energy Sciences (Award No. DE-SC0002613), the EIEG program (F.S.U.), the AFOSR MURI program, NSERC, and CIFAR. We are grateful for the local technical support at TRIUMF during the dilution fridge experiments at M15.

*Present address: Department of Physics, Ewha University, Seoul, South Korea, 120–750.

†Present address: Department of Chemistry, University of Winnipeg, Winnipeg, MB, Canada R3B 2E9. cwiebe@magnet.fsu.edu

¹S. N. Bose, *Z. Phys.* **26**, 178 (1924).

²A. Einstein, *Sitzungsber. Preuss. Akad. Wiss., Phys. Math. Kl.*, 261 (1924).

³F. London, *Nature (London)* **141**, 643 (1938).

⁴For a review, see L. P. Pitaevskii and S. Stringari, *Bose-Einstein Condensation* (Clarendon Press, Oxford, 2003).

⁵E. M. Lifshitz and L. P. Pitaevskii, *Statistical Physics Part 2* (Nauka, Moscow, USSR, 1978), Chap. 26.

⁶T. M. Rice, *Science* **298**, 760 (2002).

⁷Ch. Rüegg, N. Cavadini, A. Furrer, H.-U. Gudel, K. Krämer, H. Mutka, A. Wildes, K. Habicht, and P. Vorderwisch, *Nature (London)* **423**, 62 (2003).

⁸I. Affleck, *Phys. Rev. B* **43**, 3215 (1991).

⁹T. Giamarchi, C. Ruegg, and O. Tchernyshyov, *Nat. Phys.* **4**, 198 (2008).

¹⁰O. Mentré, A. C. Dhaussy, F. Abraham, E. Suard, and H. Steinfink, *Chem. Mater.* **11**, 2408 (1999).

¹¹T. Waki, Y. Morimoto, C. Michioka, M. Kato, H. Kageyama, K. Yoshimura, S. Nakatsuji, O. Sakai, Y. Maeno, H. Mitamura, and

T. Goto, *J. Phys. Soc. Jpn.* **73**, 3435 (2004).

¹²J. Hall, W. Marsh, R. Weller, and W. Hatfield, *Inorg. Chem.* **20**, 1033 (1981).

¹³D. C. Johnston, R. K. Kremer, M. Troyer, X. Wang, A. Klümper, S. L. Büdke, A. F. Panchula, and P. C. Canfield, *Phys. Rev. B* **61**, 9558 (2000).

¹⁴E. C. Samulon, Y. J. Jo, P. Sengupta, C. D. Batista, M. Jaime, L. Balicas, and I. R. Fisher, *Phys. Rev. B* **77**, 214441 (2008).

¹⁵W. Higemoto, H. Tanaka, I. Watanabe, S. Ohira, A. Fukaya, and K. Nagamine, *Physica B* **289**, 172 (2000).

¹⁶N. Cavadini, D. Andreica, F. N. Gygax, A. Schenck, K. Krämer, H.-U. Fudel, H. Mutka, and A. Wildes, *Physica B* **335**, 37 (2003).

¹⁷T. Suzuki, I. Watanabe, A. Oosawa, T. Fujiwara, T. Goto, F. Yamada, and H. Tanaka, *J. Phys. Soc. Jpn.* **75**, 025001 (2006).

¹⁸T. Suzuki, F. Yamada, I. Watanabe, T. Goto, A. Oosawa, and H. Tanaka, *J. Phys. Soc. Jpn.* **76**, 074704 (2007).

¹⁹T. Nikuni, M. Oshikawa, A. Oosawa, and H. Tanaka, *Phys. Rev. Lett.* **84**, 5868 (2000).

²⁰F. Yamada, T. Ono, H. Tanaka, G. Misguich, M. Oshikawa, and T. Sakakibara, *J. Phys. Soc. Jpn.* **77**, 013701 (2008).

²¹M. Crisan, I. Tifrea, D. Bodea, and I. Grosu, *Phys. Rev. B* **72**, 184414 (2005).